BULLETIN OF THE POLISH ACADEMY OF SCIENCES
TECHNICAL SCIENCES, Vol. 70(2), 2022, Article number: e140259
DOI: 10.24425/bpasts.2022.140259

A method of point cloud data block registration with considering distance from point to surface

Yinju LU[1,2]*, Mingyi DUAN[2], and Shuguang DAI[1]

[1] School of Optical Electrical and Computer Engineering, University of Shanghai for Science and Technology, Shanghai 200093, China
[2] School of Information Engineering, Zhengzhou Institute of Technology, Zhengzhou 450044, China

Abstract. The number of scanner stations used to acquire point cloud data is limited, resulting in poor data registration. As a result, a cloud point block registration approach was proposed that took into account the distance between the point and the surface. When registering point cloud data, the invariant angle, length, and area of the two groups of point cloud data were affine transformed, and then the block registration parameters of point cloud data were determined. A finite hybrid model of point cloud data was created based on the coplane four-point nonuniqueness during the affine translation. On this basis, the point cloud data block registration algorithm was designed. Experimental results prove that the proposed method has great advantages in texture alignment, registration accuracy and registration time, so it is able to effectively improve the registration effect of point cloud data. The point cloud data block registration algorithm was built on this foundation. Experiments show that the suggested method has significant improvements in texture alignment, registration accuracy, and registration time, indicating that it can significantly improve point cloud data registration.

Key words: point cloud registration; data block registration; distance from point to surface; parameter calculation.

1. INTRODUCTION

With continuous updating of point cloud acquisition technology and continuous improvement of measurement means, the storage quantity of point cloud data is also greatly increased. The point clouds collected by single station can research 100 000 or one million, and the distribution of point clouds is different. Before modeling the massive point cloud data, it is necessary to preprocess the point cloud and thus to ensure the robustness and timeliness of model [1]. Meanwhile, the point cloud registration is the most important link. The accuracy and efficiency of registration influence the final results.

Point cloud registration is unifying the point cloud data obtained by multiple stations into the same coordinate system, and then build a complete point cloud data model [2]. In the actual process of data acquisition, single station measurement is difficult to conduct all-round data acquisition for the object to be measured, especially when the surface structure of an object is complex, or the volume is relatively large [3]. The registration process of point cloud data is to align the point clouds of multiple stations in the same coordinate system, so as to calculate the 3D geometric model of an object.

Since the 1990s, the continuous updating of point cloud registration algorithm has provided a variety of materials for researchers. Z. Lanming [4] proposed a registration method for the point cloud data on a rotating platform. Firstly, the central axis of the rotating platform was calibrated by three-point clouds with different angles on the cylindrical surface, so that the relative relationship between the scanning equipment and the rotating platform could be obtained. Then, the rotation matrix between multiple point clouds was calculated by the angle of the rotating platform. Finally, the point clouds obtained from any angle were registered in a unified coordinate system. This method only used the rotation angle of a platform to construct the rotation matrix and thus to realize automatic registration. Moreover, this method was stable and efficient. Its stitching accuracy is equivalent to that of iterative closest point (ICP) registration method and marker registration method. It was used with laser scanners or structure light scanners. L. Xiaoyan [5] used the micro tangent plane to estimate the normal vector of scattered point cloud data and adjusted the normal vector direction globally. The stable quadric surface fitting method was used to estimate the Gaussian curvature and mean curvature of point cloud data. The coordinates, normal vectors and curvature of points were combined into 8-dimensional feature vectors. The vectors with similar geometric features were combined into one group by fuzzy maximum likelihood estimation clustering technology. Thus, the segmentation of point cloud data was completed. W. Xia [6] developed a point cloud registration method based on overlapping region. Firstly, the point cloud was divided into some blocks by the angle between normal lines and curvature features with distance weight, and then multi-dimensional feature descriptor of point cloud block was constructed. By comparing the similarity of variance distribution between point cloud blocks, the overlapping region of adjacent point clouds was extracted. Then, the point cloud in the overlapping region was brought into the super four-point fast robust matching algorithm for registration. According to the

*e-mail: luyinju2019@126.com

Manuscript submitted 2021-05-13, revised 2021-07-04, initially accepted for publication 2021-08-24, published in April 2022.

consistency constraint, the optimal rigid transformation matrix was applied to the original data and thus to build the point cloud registration model, so as to enhance the registration accuracy. J.H. Xiao [7] proposed a 3D point cloud registration method without odometer based on area attribute. This method only needs to extract the area of each segment and plane parameters, without the prior attitude estimation of sensors. R. Lai [8] proposed a computational model and a point cloud registration algorithm based on non-rigid transformation. Firstly, the leading feature values and feature functions of LB operators which were inherently defined on manifolds. Secondly, the original point clouds were transformed into the point clouds embedded in Euclidean space by Laplace-Beltrami feature mapping. The LB feature map was invariant under the isometric transformation of the primitive manifold. On this basis, the model and algorithm of point cloud registration in the form of distribution/probability was designed based on the optimal transmission theory.

Although 3D scanning technology based on point cloud data is ahigh precision, high efficiency and high-tech measurement method, there are still many challenges [9–11]. Based on the above background, the point cloud registration is not only the key technology of processing point cloud data, but also an important part of reverse engineering, which provides technical support for 3D modeling of reverse engineering. In the face of massive point cloud data, it is necessary to research a method of point cloud registration with high precision and high efficiency to meet the different requirements of projects. Therefore, a new method of point cloud data block registration based on the point to surface distance was put forward.

2. DESIGN OF BLOCK REGISTRATION METHOD FOR POINT CLOUD DATA

2.1. Calculation of point cloud data block registration parameters

The finite hybrid model of point cloud data block registration is built by rigid body transformation in 3D transformation [12–14]. The essence of rigid body transformation is to rotate and translate the object in 3D space, and keep the gradient, divergence, and curl unchanged. In the process of data registration, two groups of point cloud data need to be transformed into the same coordinate system by rigid body transformation, so that the affine transformation with invariable angle, length and area can be carried out. The affine transformation H is defined by equation (1)

$$H = \begin{bmatrix} r_{11} & r_{12} & r_{13} & t_x \\ r_{21} & r_{22} & r_{23} & t_y \\ r_{31} & r_{32} & r_{33} & t_z \\ v_x & v_y & v_z & S \end{bmatrix}. \tag{1}$$

Equation (1) can also be converted into (2):

$$H = \begin{bmatrix} R & T \\ V & S \end{bmatrix}. \tag{2}$$

In equation (2), $R = \begin{bmatrix} r_{11} & r_{12} & r_{13} \\ r_{21} & r_{22} & r_{23} \\ r_{31} & r_{32} & r_{33} \end{bmatrix}$ is the rotation matrix. $T = \begin{bmatrix} t_x \\ t_y \\ t_z \end{bmatrix}$ is the translation matrix. $V = \begin{bmatrix} v_x \\ v_y \\ v_z \end{bmatrix}^T$ is the perspective transformation matrix. S is the transformation scale.

After the rigid body transformation, the point cloud is only rotated and translated without deformation. The point cloud data rotates around X axis, Y axis and Z axis.

When it rotates around X-axis:

$$R_X(\theta) = \begin{bmatrix} 1 & 0 & 0 \\ 0 & \cos\theta & \sin\theta \\ 0 & \sin\theta & \cos\theta \end{bmatrix}. \tag{3}$$

When it rotates around Y-axis:

$$R_Y(\theta) = \begin{bmatrix} \cos\theta & 0 & \sin\theta \\ 0 & 1 & 0 \\ -\sin\theta & 0 & \cos\theta \end{bmatrix}. \tag{4}$$

When it rotates around Z-axis:

$$R_Z(\theta) = \begin{bmatrix} \cos\theta & -\sin\theta & 0 \\ \sin\theta & \cos\theta & 0 \\ 0 & 0 & 1 \end{bmatrix}. \tag{5}$$

The translation along X axis, Y axis and Z axis is:

$$T_{(3\times1)} = \begin{bmatrix} t_x \\ t_y \\ t_z \end{bmatrix}. \tag{6}$$

The source point cloud set R and target point cloud set Q are transformed by rotation matrix R and translation matrix T, and the point cloud set Q' is obtained.

$$Q = R_{(3\times3)} \times P + T_{(3\times1)}. \tag{7}$$

After transforming (3) to (7), the rotation matrix $R_{3\times3}$ can be obtained.

$$R_{(3\times3)} = \begin{bmatrix} r_{11} & r_{12} \\ r_{21} & r_{22} \\ r_{31} & r_{32} \end{bmatrix}, \tag{8}$$

where

$$\begin{aligned} r_{11} &= \cos\beta\cos\gamma, \\ r_{12} &= \cos\beta\sin\gamma, \\ r_{21} &= -\cos\alpha\sin\gamma - \sin\alpha\sin\beta\cos\gamma\cos\alpha\cos\gamma \\ &\quad + \sin\alpha\sin\beta\sin\gamma, \\ r_{22} &= \sin\alpha\cos\beta, \\ r_{31} &= \sin\alpha\sin\gamma + \cos\alpha\sin\beta\cos\gamma, \\ r_{32} &= -\sin\alpha\cos\gamma - \cos\alpha\sin\beta\sin\gamma\cos\alpha\cos\beta. \end{aligned}$$

According to (8), if we want to get the value of $R_{3\times3}$, it is necessary to find the value of six unknown numbers (α, β, γ, t_x, t_y, t_z). At least six linear equations should be determined. Meanwhile, at least three-point pairs that are not on the same line should be determined in the overlapping region of two groups of point clouds. Finally, the values of six unknown parameters can be calculated to solve the rigid transformation matrix [15–17].

2.2. Build a finite hybrid model of point cloud data

The overlapped region in point cloud data is regarded as the initial data of registration, which is marked as P_c and Q_c. In point cloud P_c, three points are randomly selected, and then the fourth point is selected to make the four points on the same plane, which is marked as $B = \{p_1, p_2, p_3, p_4\}$. In the process of selecting these points, the distance among four points should be as large as possible, and the four points must fall in the overlapping region at the same time. Therefore, the overlapping region is taken as the initial data to meet this condition.

In order to find the coplanar four-point set U which is nearly congruent with B in point cloud data Q_c, the distance and cross ratio of two lines in B are calculated by equations (9) and (10). According to the constraints of consistent distance and consistent cross ratio, all coplanar four-point sets $U = \{U_1, U_2, U_3, \ldots, U_n\}$ satisfying the conditions are found in point cloud Q_c. For each U_i, the rigid transformation matrix is solved according to the correlation information between B and U_i, and then the rigid transformation with the best registration accuracy is selected as the final global registration parameter by comparing and maximizing the common point sets.

$$d_1 = \|p_2 - p_1\|, \qquad d_2 = \|p_4 - p_3\|, \tag{9}$$

$$\lambda_1 = \frac{\|p_1 - o_1\|}{d_1}, \qquad \lambda_2 = \frac{\|p_3 - o_1\|}{d_2}. \tag{10}$$

In Fig. 1, $\{q_1, q_2, q_3, q_4\}$ and $\{q_1', q_2', q_3, q_4\}$ are alternate four-point bases under the conditions. Obviously, the latter is not a congruent coplanar four-point basis, which leads to the increase of matching time cost. On this basis, the finite hybrid model of point cloud data introduces the angle consistent constraint $\angle p_1 o_1 p_3 = \angle q_1 o_2 q_3$, which greatly reduces the number of candidate coplanar four-point bases, and thus increasing the matching accuracy.

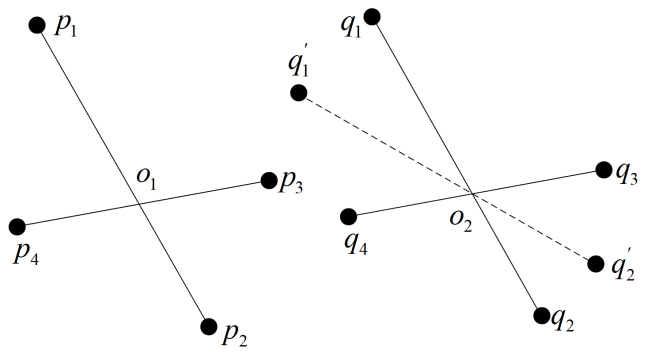

Fig. 1. Nonuniqueness of coplanar four-point base under affine transformation

Based on the above analysis, the establishment of finite hybrid model of point cloud data is described as follows:

Step 1: according to the distance (d_1, d_2) between the line segments of coplanar four-point base given by B, we can find the point pair sets (R_1, R_2) with the distance $d_1 \pm \varepsilon$ and $d_2 \pm \varepsilon$ in the point cloud Q_c respectively;

Step 2: construct a three-dimensional grid G with size of ε, and rasterize the surface of point cloud [18];

Step 3: for $p_1p_2(p_2p_1)$ and $p_3p_4(p_4p_3)$, traverse all candidate point pairs in R_1 and R_2, calculate all cross nodes by cross-ratio consistency, store them in grid Gand normalize the vectors at the same time;

Step 4: suppose that the angle between the two-point pairs is θ, according to the intersection point stored in grid G and the corresponding vector index, all the included angles are θ. They are matched by four-point based within error range of ξ [19].

According to the nonuniqueness of coplanar four-point base under affine transformation, the finite hybrid model of point cloud data is built. Next, the block registration algorithm of point cloud data is designed to realize the block registration.

2.3. Block registration of point cloud data

In general, the point cloud data to be registered are partially overlapped, the registration algorithm based on global geometric invariants is difficult to directly provide good initial position for it. Theoretically, we can find the overlapped part of point cloud data at first, but it is not easy to find the overlap part [20, 21]. In order to quickly make the relative position of point cloud data be approached, the distance from point to surface is adopted as the initial registration of point cloud data, and then accurate registration is adopted to improve the registration accuracy and efficiency. The flow of algorithm is shown in Fig. 2.

RGB-D data of color object is collected by Kinect. Before registration, the source point and target point clouds are read, and then the color RGB mode is converted to the gray mode. As given in Fig. 2 gray range is mapped to depth range mixed feature. Meanwhile, the repeated points are deleted. Moreover, the two-point clouds to be registered are quickly closed by the principal direction application algorithm [22]. The principal direction application algorithm mainly calculates the variance matrix of the two-point clouds, and thus to get the eigenvectors and feature values corresponding to the covariance matrices. Taking the center of gravity of point cloud as the origin, we can build he reference coordinate system based on eigenvector, and then get the coordinate transformation matrix by the unit quaternion method. Next, the feature points are obtained based on the mixed features. According to the points corresponding to the search feature points (x, y, z, gray), The corresponding point pairs are formed, and the mean value between point pairs (x, y, z, gray) is calculated. The point pairs that are bigger than the mean value are eliminated. The point pairs are iterated until the conditions are met. The optimal rotation matrix R and translation direction T are obtained. Thus, the block registration of point cloud data is completed.

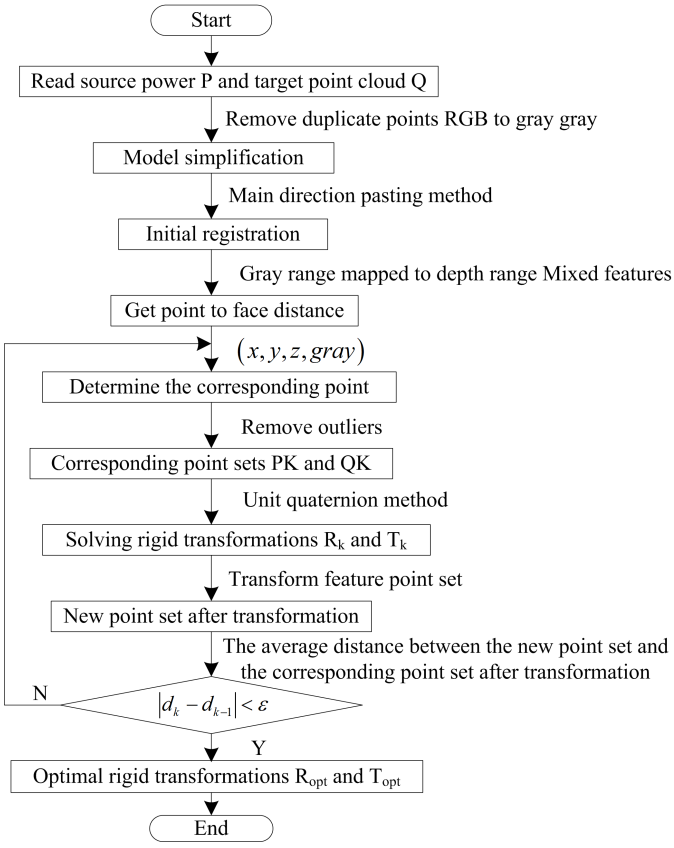

Fig. 2. The flow of block registration algorithm of point cloud data

3. IMPLEMENTATION OF POINT CLOUD DATA BLOCK REGISTRATION

The block registration of point cloud data includes two stages: initial registration and accurate registration. The initial registration is to provide a good initial position for accurate registration, and the accurate registration algorithm is used to further improve the registration accuracy.

3.1. Extraction of distance from point to surface in point cloud data

In the precise registration process, the point-to-surface distance is used to search the corresponding points. The rigid transformation is calculated to change the position of point cloud. Reducing the time in each iteration will reduce the overall registration time. The point-to-surface distance can also show the key information of point cloud. In the iterative process of accurate registration, the point-to-surface distance is adopted for iterative registration. The number of points in different point cloud data is different, so the number of distances extracted is different. The mixed features of source point cloud are arranged from large to small, and 20% of the point-to-surface distance is extracted to approximately describe the whole point cloud.

3.2. Selection of points

KNN algorithm and $(x, y, z, [gray)$ are adopted to search for the corresponding points of the distance from point to surface. The process is to calculate the minimum 2 norm of 4D descriptors between point sets and thus to obtain the corresponding points and establish corresponding point sets. Some point pairs with large distance are eliminated. Due to the limited range of depth data collected by Kinect, the range of gray value obtained by RGB conversion is much larger than the range of depth data. During the calculation of Euclidean distance, it is necessary to keep the rage of gray value consistent with the rage of depth value and map the rage of gray value to the rage of depth value by equation (11).

$$\text{gray}' = \frac{d_{\text{mix}} - d_{\text{min}}}{gray_{\text{max}} - gray_{\text{min}}} (\text{gray} - \text{gray}_{\text{min}}) + d_{\text{min}}. \quad (11)$$

4D search space is 3D geometry data and gray value after mapping. That is (x, y, z, gray'). The color information is added to the search space to assist geometric information to search for more accurate points. The point-to-face distance coordinates in source point cloud are transformed into $(x_i, y_i, z_i, \text{gray}'_i)$. The corresponding points of the point-to-surface distance in point cloud data by equation (12).

$$r_{ij} = \sqrt{(x_i - x_j)^2 + (y_i - y_j)^2 + (z_i - z_j)^2 + \left(\text{gray}'_i - \text{gray}'_j\right)^2}. \quad (12)$$

In (12), $(x_j, y_j, z_j, \text{gray}'_j)$ represents the geometric coordinates of all points in target point cloud data and the color value after transformation. Formula (12) is used to find out the closest point of the point-to-surface distance in target point cloud as the corresponding point. That is to search the point with the minimum value of 4D Euclidean distance in target point cloud as the corresponding point.

After the corresponding points are searched by 4D, the corresponding points and the distance from point to surface constitute the point pair set. In order to better calculate the rigid transformation, we should eliminate the corresponding point pairs which are too large in 4D space and calculate the Euclidean distance of the corresponding set of point pairs in 4D space. The mean value of Euclidean distance is μ_f. We can take the point pair less than the mean value, and then 4D-ICP iteration continues.

3.3. 4D-ICP Iterative Process

In the iterative process, the data mode of the distance from point to surface and the corresponding point is 4D (3D geometric data and gray value mapped to the geometric range). The specific steps are described as follows:

Input: the distance from point to surface and the target point cloud.

Output: optimal rotation matrix and translation vector.

Step 1: Set the number of iterations N;

Step 2: While $i < N$ & $em_i > 1 \times 10^{-7}$;

Step 3: Use KNN algorithm to search the nearest point in the target point cloud of 4D space and eliminate the error point pair by Euclidean distance threshold method. The mean value of corresponding point pair on space $(x, y, z, gray)$ is calculated, and the point pair less than the mean value is selected;

Step 4: Use the unit quaternion method to solve the rotation matrix and translation vector between the remaining point pairs and calculate the root mean square error of the point pair;

Step 5: $em_i = \left|\mathrm{RMSE}_i - \mathrm{RMSE}_{i-1}\right|, i = 2, \ldots, N$;

Step 6: Apply the rotation matrix and translation vector to the point-to-face distance set and then update the position of distance set;

Step 7: Until the condition is met, otherwise the iteration continues.

The 4D-ICP iteration mainly aims at the point cloud registration of low-quality RGB-D data with high noise collected by Kinect. In the accurate registration stage, the color information is added for 4D-ICP iterative registration. In the low-quality and high-noise RGB-D data, the point-to-surface distance is obtained by mixed features. Correspondingly, the points are searched by 4D descriptor during the iteration so that the points are more accurate. Moreover, RGB information is added for 4D search to improve the accuracy of the corresponding points. Therefore, the point-to-surface distance is used to improve the accuracy, and thus to accelerate the iterative convergence.

4. EXPERIMENTAL RESULTS

To validate the effectiveness of the method that considers the distance from point to surface, an experiment was designed.

Due to the lack of public RGB-D data set, the low-precision RGB-D data collected by Kinect was used to validate the effectiveness of the method with considering the distance from point to surface. The data model includes two David models and two pillow models.

To demonstrate the effectiveness of the proposed method in point cloud registration, the classic ICP registration method, the improved ICP registration method based on curvature feature point and 4D-ICP registration method were compared.

The experimental object is a single-color object. The comparison results of four groups of experiments are shown in Figs. 3, 4, 5, and 6, where (a) denotes the initial relative position of the two-point clouds that need to be registered. Four different registration methods (b), (c), (d), (e) are to make the two-point clouds in (a) make approach each other by the initial registration, so as to provide good space initial position for the iteration of accurate registration. However, the accurate registration part is different. (b) is to use the classical ICP method to search for all the point clouds in the iteration process, and then the minimum distance between the three-dimensional points is used as the corresponding points to perform the iteration. (c) is the improved ICP method. In the iteration process, the 3D-ICP point cloud registration method based on curvature feature points is used to obtain 20% of the feature points, and then the curvature feature points are used to search, and then the minimum distance between the three-dimensional points is used as the corresponding points to perform the iteration. (d) is the iterative registration results of 4D-ICP method. All the points in source cloud, the corresponding points are searched by (x, y, z, gray) composed of the depth data and the hue in HSL color mode. After that, 4D-ICP iteration is carried out. (e) is the registration result of the proposed method. The mixed features are used to

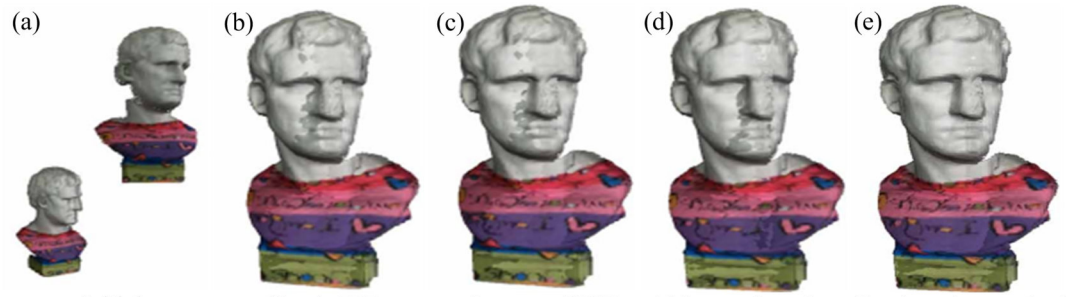

Fig. 3. Registration effect of different registration methods on david model 1

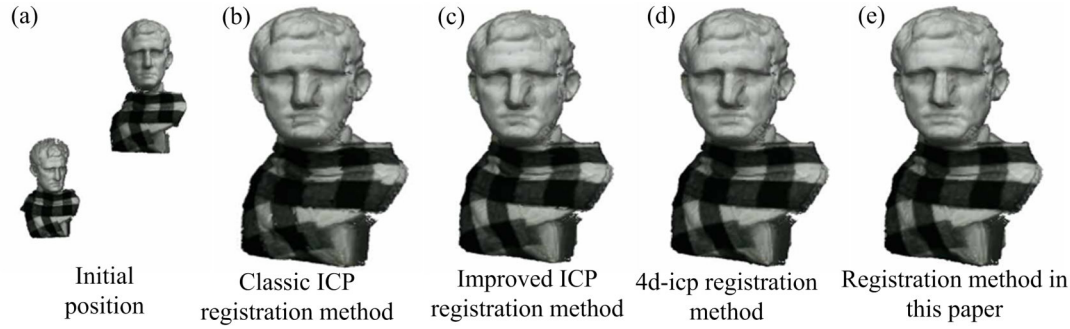

Fig. 4. Registration effect of different registration methods on david model 2

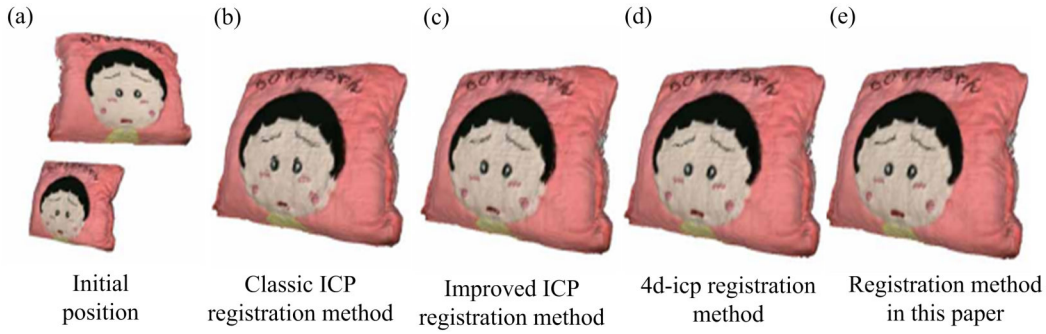

Fig. 5. Registration effect of different registration methods on pillow model 1

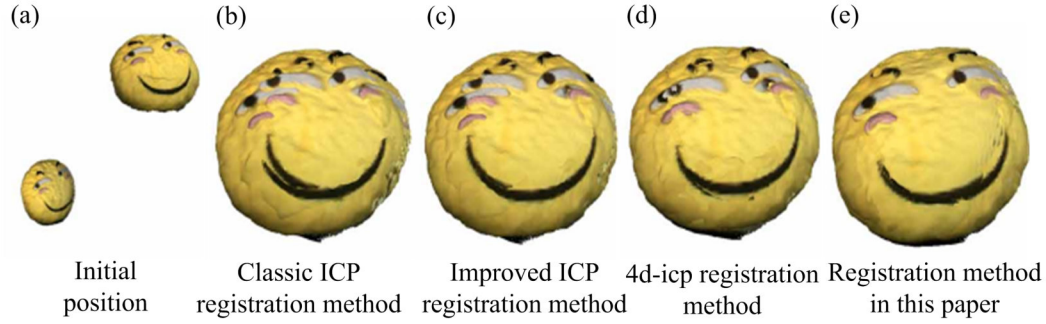

Fig. 6. Registration effect of different registration methods on pillow model 2

get the feature points. The number of feature points is 20% of the points of source point could. The corresponding points of feature points are searched by (x, y, z, gray) composed of the geometric data and the color data converted from RGB mode to gray mode.

5. DISCUSSION

To further understand comparison results, the iteration times, registration time and global color error of all methods were compared. The number of iterations shows that each algorithm has the same stop condition of iteration error when the error stop condition is reached. The registration time is from the precise registration to the optimal rigid transformation. In the measurement of registration error, there may be the corresponding deviation between point pairs, and the best registration refers to the good registration between color and texture. The global color error is to search the nearest point of Euclidean distance of RGB data in target point cloud by the transformed source point cloud, and calculate the root mean square error between the transformed source point cloud and its nearest point.

The global color error and registration time of different methods on each model are compared in the column chart and the line chart respectively, and then the results are shown in Figs. 7 and 8.

Compared with Table 1 and Fig. 7, we can see that the point cloud data block registration method considering the point-to-face distance has the smallest global color error than the other methods. Moreover, the comparison of registration results proves good registration effect of the proposed method.

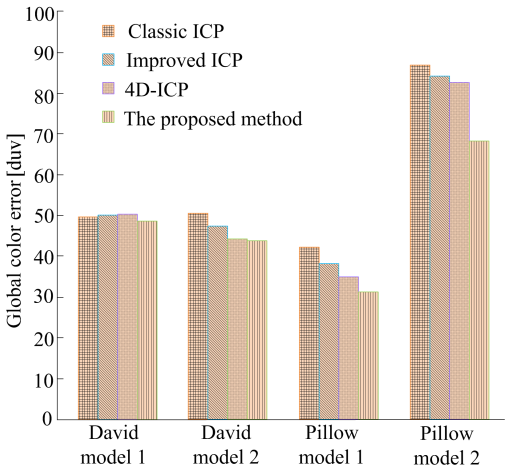

Fig. 7. Global distribution of color error of different registration methods on different models

In terms of registration time, Table 1 and Fig. 8 show that in the color David model, black-and-white David model and pillow model, 3D-ICP method and 4 D-ICP method use all points in source point cloud to search corresponding points during the iteration, but the improved ICP and the proposed method use feature points to search corresponding points, so the running time of the proposed method is reduced, which is better than 3D-ICP method and 4 D-ICP method. Meanwhile, the proposed method has advantages in running time of other methods of searching corresponding points by feature points. For the pillow model 2, after comparing with the registration effect in Fig. 6

Table 1
Comparison of four methods of block registration for point cloud data

Registration model	Number of point clouds	Number of deleted duplicate points	Registration method	Number of iterations / times	Registration time / s	Global color error / duv	Registration effect
David model 1	120631	20387	ClassicICP	161	17.7235	49.8052	Fig. 3b
			Improved ICP	154	8.3427	50.0112	Fig. 3c
	116847	19778	4D-ICP	107	15.3436	50.2114	Fig. 3d
			The proposed method	100	6.8474	48.6082	Fig. 3e
David model 2	140057	24034	ClassicICP	124	16.1423	50.4238	Fig. 4b
			Improved ICP	117	7.3358	47.3204	Fig. 4c
	134314	22909	4D-ICP	86	18.2052	44.4927	Fig. 4d
			The proposed method	68	5.5377	44.0261	Fig. 4e
Pillow model 1	174106	29216	ClassicICP	92	11.7359	42.3426	Fig. 5b
			Improved ICP	42	4.1295	38.3378	Fig. 5c
	157488	26387	4D-ICP	58	9.9268	34.9757	Fig. 5d
			The proposed method	19	3.0359	31.2352	Fig. 5e
Pillow model 2	82437	14079	ClassicICP	41	2.8497	87.1143	Fig. 6b
			Improved ICP	47	2.4495	84.1447	Fig. 6c
	80783	13682	4D-ICP	192	19.9205	82.7664	Fig. 6d
			The proposed method	125	5.2762	68.3915	Fig. 6e

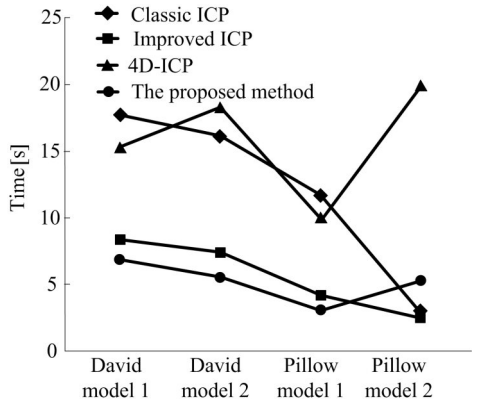

Fig. 8. Running time of different registration methods on different models

and the data in Table 1, we can see that other methods have advantages in terms of registration time, but the registration effect is not good. Although the running time of the proposed method is not as good as other methods, it is superior to other methods in registration effect and global color error.

The registration results of two David models and two pillow models show that the proposed method has good registration results for color information model and black-and-white texture model, or RGB-D model whose geometry structure is not complicated enough. Based on the overall experimental results, the proposed method is effective in low-precision RGB-D data registration. Compared with other improved ICP methods, the proposed method has advantages in texture alignment, registration accuracy and registration time.

6. CONCLUSIONS

This paper proposes a block registration approach for point cloud data that takes into account the distance between point and surface. The operation time of this method is slightly slower than that of other ways, according to experimental results. The proposed technique outperforms existing methods in terms of the diagram's registration effect and the global color error in the table. However, the proposed method's registration effect is primarily determined by the extraction effect of overlapping regions. Extracting overlapping regions for a data model with a complicated surface is difficult, and the registration accuracy suffers as a result. In the future, more efficient methods for extracting overlapping regions will need to be investigated in order to improve the accuracy and universality of the point cloud registration approach.

ACKNOWLEDGEMENTS

The research is supported by Henan Province Science and Technology Project (Key Science and Technology Program of Henan Province, China), Project No. 192102210120.

REFERENCES

[1] K. Zampogiannis, C. Fermuller, and Y. Aloimonos, "Topology-aware non-rigid point cloud registration", *IEEE Trans. Pattern Anal. Mach. Intell.*, vol. 34, no. 99, pp. 1–12, 2019.

[2] E. Renaudin, A. Habib, and A.P. Kersting, "Featured-based registration of terrestrial laser scans with minimum overlap using photogrammetric data", *ETRI J.*, vol. 33, no. 4, pp. 527, 2011.

[3] S. Chen, L. Nan, R. Xia, and Z.B. Zhao, "PLADE: A plane-based descriptor for point cloud registration with small overlap", *IEEE Trans. Geosci. Remote Sens.*, vol. 58, no. 4, pp. 2530–2540, 2020.

[4] L.M. Zhou, S.Y. Zheng, and R.Y. Huang, "A registration algorithm for point clouds obtained by scanning objects on turntable", *Acta Geod. Cartograph. Sinica*, vol. 42, no. 1, pp. 73–79, 2013.

[5] X.Y. Liu, "Point-cloud data segmentation based on fuzzy maximum likelihood estimate clustering", *Comput. Eng.*, vol. 36, no. 6, pp. 86–88, 2010.

[6] X. Wang, Y.D. Zhao, and J. Wang, "A registration method of laser point cloud with low overlap", *Sci. Surv. Mapp.*, vol. 43, no. 12, pp. 130–136, 2018.

[7] J.H. Xiao, B. Adler, J.W. Zhang, and H.X. Zhang, "Planar segment based three-dimensional point cloud registration in outdoor environments", *J. Field Robot.*, vol. 30, no. 4, pp. 552–582, 2013.

[8] W.M. Zhang, and Y.X. Zhang, "The reactive power and voltage control management strategy based on virtual reactance cloud control", *Arch. Electr. Eng.*, vol. 69, no. 4, pp. 921–936, 2020.

[9] Y.R. Hou, "Optimal error estimates of a decoupled scheme based on two-grid finite element for mixed stokes-darcy model", *Appl. Math. Lett.*, vol. 57, no. 12, pp. 90–96, 2016.

[10] J. Wang, S. Huo, Y. Liu, R. Li, and Z. Liu, "Research of fast point cloudregistration method in construction erroranalysis of hull blocks", *Int. J. Nav. Archit. Ocean Eng.*, vol. 12, pp. 605–616, 2020.

[11] Y. Wang, J. Xiao, L. Liu, Y. Wang, "Efficient rock mass point cloud registration based on local invariants", *Remote Sens.*, vol. 13, pp. 1–19, 2021. doi: 10.3390/rs13081540.

[12] M. Zaborowski, "Data processing in self-controlling enterprise processes", *Bull. Pol. Acad. Sci. Tech. Sci.*, vol. 67, no. 1, pp. 1–18, 2019.

[13] F. Wang, J. Xiao, and Y. Wang, "Efficient rock-mass point cloud registration using n-point complete graphs", *IEEE Trans. Geosci. Remote Sens.*, vol. 18, no. 99, pp. 1–12, 2019, doi: 10.1109/TGRS.2019.2926201.

[14] J. Li, H. Liu, and L. Rondi, "Regularized transformation-optics cloaking for the Helmholtz equation: from partial cloak to full cloak", *Commun. Math. Phys.*, vol. 335, no. 2, pp. 671–712, 2015.

[15] N. Vaysfeld and Z. Zhuravlova, "On one new approach to the solving of an elasticity mixed plane problem for the semi-strip", *Acta Mech.*, vol. 226, no. 12, pp. 4159–4172, 2015, doi: 10.1007/s00707-015-1452-x.

[16] H. Hong and B.H. Lee, "Key-layered normal distributions transform for point cloud registration", *Electr. Lett.*, vol. 51, no. 24, pp. 1986–1988, 2015.

[17] L. Han, L. Xu, and D. Bobkov, "Real-time global registration for globally consistent RGB-D SLAM", *IEEE Trans. Robot.*, vol. 16, no. 2, pp. 1–11, 2019.

[18] X. Ge and B. Wu, "Contextual global registration of point clouds in urban scenes", *Photogramm. Eng. Remote Sens.*, vol. 85, no. 8, pp. 559–571, 2019.

[19] F. Pomerleau, M. Liu, and F. Colas, "Challenging data sets for point cloud registration algorithms", *Int. J. Robot. Res.*, vol. 31, no. 14, pp. 1705–1711, 2012.

[20] X. Huang, J. Zhang, and L. Fan, "A systematic approach for cross-source point cloud registration by preserving macro and micro structures", *IEEE Trans. Image Process.*, vol. 25, no. 7, pp. 1–15, 2017.

[21] T.R. Yugo *et al.*, "3D reconstruction and multiple point cloud registration using a low precision RGB-D sensor", *Mechatronics*, vol. 35, no. 1, pp. 11–22, 2016, doi: 10.1016/j.mechatronics.2015.10.014.

[22] G.K. Saini *et al.*, "Recognition of human sentiment from image using machine learning", *Ann. Rom. Soc. Cell Biol.*, vol. 25, no. 5, pp. 1802–1808, 2021.